Master Sciences de la Matière
École normale supérieure de Lyon
Université Claude Bernard Lyon 1

Phase Transitions and Critical Phenomena
Yann-Edwin KETA
M2 Physique – 2017-2018

Nematic order in packings of spheroids

Abstract: *We first give evidence of a density-driven isotropic-nematic transition of first order in static packings of hard-core spheroids, based on results derived from recent theoretical developments by Nascimento et al. We then investigate the effect of the jamming transition on the orientational order in sheared packings of soft-core spheroids based on numerical simulations.*

Contents

Introduction

Granular materials are composed of athermal – *i.e.*, thermal agitation does not affect the kinetic energy of the system –, macroscopic objects – *i.e.*, they can be observed with the naked eye. [1] They are qualified as soft-matter, since they can show either liquid-like or solid-like properties under different experimental conditions.

Despite their ubiquity in nature and the fact that they are the second-most manipulated material in industry [2], little was known about granular materials until a few decades ago. According to Pierre-Gilles de Gennes, "granular matter in 1998 [was] at the level of solid state physics in 1930." [3] Yet, these materials are of great theoretical interest in the domain of statistical mechanics. Indeed, according to the own words of Leo P. Kadanoff himself, "one might even say that the study of granular materials gives one a chance to reinvent statistical mechanics in a new context." [4]

Hopefully, a lot of theoretical, numerical and experimental work has been done on the topic of granular materials since these two citations. One of the current most thrilling area of research is the jamming transition occurring in these. What has been observed is that granular materials develop a yield stress in a disordered state [5] – or a stress relaxation time which exceeds a reasonable experimental time – upon increasing the packing fraction ϕ above a critical value ϕ_J. At low ϕ, each particle can move independently of its neighbours while at high ϕ the particles can not avoid each other, resulting in a bulk modulus since the pressure increases upon compression. This phenomenon is called jamming and corresponds to a transition from a flowing liquid-like state to an amorphous rigid solid state.

Much work on the jamming transition has focused on ideal packings of disks in 2D and spheres in 3D, both theoretically [6] and numerically [7, 8]. However, early publications by Donev *et al.* [9, 10] have showed that packings of ellipsoids are of great interest. Indeed, their data showed that the value of the packing fraction in random jammed packings of ellipsoids can not only be greater than its value in spheres' random close packing (RCP), $\phi \sim 0.64$, but also close to its value in spheres' ordered face-centered cubic (fcc) or hexagonal close-packed (hcp) packings, $\phi \sim 0.74$, which is the highest value possible for packings of spheres. In crystal packings of ellipsoids, the value of $\phi \sim 0.77$ was even obtained. [11] Determining and characterising the densest possible packings is of great physical interest. For hard particles, the densest packed phase is the most thermodynamically stable at high density. Therefore, if hard particles – such as the aforementioned ellipsoids – were to pack more densely in a random configuration rather than in a crystal array, these would not crystallise. [12]

Contrarily to spheres, ellipsoids are anisotropic particles. Therefore, when studying packings of ellipsoids, one might be interested in their orientations. Thirty years ago, Frenkel and Mulder investigated the existence of an orientational order in packings of hard spheroids [13] – *i.e.*, ellipsoids of revolutions – inspired by the early, much celebrated, theoretical work by Onsager on packings of rigid hard rods. [14] Our first goal in this essay will be to study if and how an orientational order appears in static packings of spheroids at equilibrium.

Numerical shearing simulations of non-rotating frictionless soft-core disks have been proven particularly efficient to study the jamming transition [7, 8] and have recently been adapted by our research team at Umeå University to the study of rotating soft-core spheroids. Based on the data gathered from these simulations, our second goal in this essay will be to study what happens to the orientational order close to the jamming transition.

1 Nematic-isotropic transition in static packings of spheroids

1.1 Nematic order and order parameter

Term "nematic order" is the most often employed in the field of liquid crystals. Liquid crystals are composed of molecules with high shape-anisotropy – such as rigid rods or spheroids. Among them, thermotropic liquid crystals experience temperature-driven phase transitions between phases of different translational and orientational order (Figure 1). [15]

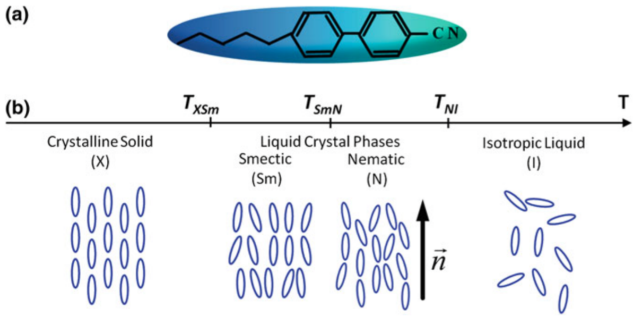

Figure 1: **(a)** Anisotropic shape of a typical liquid crystal molecule (here Pentylcyanobiphenyl), modelled as a spheroid. **(b)** Different crystal phases and domains of existence. Vector $\vec{n}$ denotes the local director field along which the orientations of the particles are aligned in the non-isotropic phases. *source:* [15], Figure 2.1

From the least ordered to the most ordered, these phases are:

$\boldsymbol{T > T_{NI}}$**:** the isotropic phase, in which the molecules are randomly oriented and positioned;

$\boldsymbol{T_{SmN} < T < T_{NI}}$**:** the nematic phase, in which the molecules are randomly positioned but are on average aligned with the vector $\vec{n}$, called the director, hence displaying an orientational order;

$\boldsymbol{T_{XSm} < T < T_{SmN}}$**:** the smectic phase, in which the molecules are segregated into planes and conserve the orientational order of the nematic phase;

$\boldsymbol{T < T_{XSm}}$**:** the crystalline solid, in which the molecules are perfectly ordered, both in orientation and position.

To distinguish the isotropic and nematic phases, and also quantify the orientational order in the nematic phase, we need to introduce a nematic order parameter.

Consider a packing of identically shaped particles. For a matter of simplicity, we will assume these particles have a symmetry axis, therefore for any given particle there exists $\vec{I} \in \mathbb{S}^2$ such that the particle has cylindrical symmetry around $\vec{I}$. First of all, we introduce the orientation descriptor

$$\boldsymbol{\sigma}(\vec{I}) = \frac{1}{2}\left(3\vec{I} \otimes \vec{I} - \mathbb{1}\right) \tag{1}$$

such that $\vec{I}$ is an eigenvector of $\boldsymbol{\sigma}(\vec{I})$ associated to the eigenvalue 1 and $\boldsymbol{\sigma}(\vec{I})$ is an homothety of ratio $-1/2$ on $\text{span}(\vec{I})^{\perp}$, thus leading to $\text{tr}(\boldsymbol{\sigma}(\vec{I})) = 0$. Moreover, we can notice that, by definition, $\boldsymbol{\sigma}(\vec{I})$ is real and symmetric.

We then introduce the probability distribution function of orientation, $f(\vec{I})$, such that the probability of a given particle to have its axis of symmetry aligned with $\vec{I}$ is $f(\vec{I})d^2\vec{I}$. Since f is a probability distribution function, it must satisfy the following condition

$$\int_{\mathbb{S}^2} d^2\vec{I}\, f(\vec{I}) = 1 \tag{2}$$

We finally introduce the order parameter tensor $\boldsymbol{Q}$ given by

$$\boldsymbol{Q} = \int_{\mathbb{S}^2} d^2\vec{I}\, f(\vec{I})\boldsymbol{\sigma}(\vec{I}) =< \boldsymbol{\sigma}(\vec{I}) > \tag{3}$$

which satisfies $\text{tr}(\boldsymbol{Q}) = 0$, since $\forall \vec{I} \in \mathbb{S}^2,\ \text{tr}(\boldsymbol{\sigma}(\vec{I})) = 0$, and is also real and symmetric.

By application of the spectral theorem we have that $\boldsymbol{Q}$ is diagonalisable in an orthonormal triad. We denote S its greatest eigenvalue and $\vec{n}$ the associated eigenvector, and $\vec{e_1}$ and $\vec{e_2}$ two other eigenvectors of $\boldsymbol{Q}$ which form an orthonormal triad with $\vec{n}$. Since $\text{tr}(\boldsymbol{Q}) = 0$, there exists B such that $\boldsymbol{Q}\vec{e_1} = (B - S)/2\ \vec{e_1}$ and $\boldsymbol{Q}\vec{e_2} = -(B + S)/2\ \vec{e_2}$. With all these objects being introduced, we can now rewrite $\boldsymbol{Q}$ as

$$\boldsymbol{Q} = \frac{1}{2}S\left(3\vec{n} \otimes \vec{n} - \mathbb{1}\right) + \frac{1}{2}B\left(\vec{e_1} \otimes \vec{e_1} - \vec{e_2} \otimes \vec{e_2}\right) \tag{4}$$

In the case of uniaxial nematic, *i.e.* when there is a single preferred direction of orientation, we have $B = 0$. [15] We will only consider this case from now on.

We can now show that $\vec{n}$ is the director, introduced in Figure 1, and S is the nematic order parameter we have been looking for. First of all, we have to determine the relation between S and f. We can notice that

$$\begin{aligned}\boldsymbol{\sigma}(\vec{I})\vec{n} &= \frac{1}{2}\left(3\vec{I}\otimes\vec{I} - \mathbb{1}\right)\vec{n} = \frac{1}{2}\left(3\left(\vec{I}\cdot\vec{n}\right)\vec{I} - \vec{n}\right) \\ &= \underbrace{\frac{1}{2}\left(3\left(\vec{I}\cdot\vec{n}\right)^2 - 1\right)}_{P_2(\vec{I}\cdot\vec{n})}\vec{n} + a(\vec{I})\vec{e_1} + b(\vec{I})\vec{e_2}\end{aligned}$$

where P_2 is the second Legendre polynomial. Therefore, with

$$\begin{aligned}S\vec{n} = \boldsymbol{Q}\vec{n} &= \int_{\mathbb{S}^2} d^2\vec{I}\; f(\vec{I})\boldsymbol{\sigma}(\vec{I})\vec{n} \\ &= \int_{\mathbb{S}^2} d^2\vec{I}\; f(\vec{I})P_2(\vec{I}\cdot\vec{n})\vec{n} + \int_{\mathbb{S}^2} d^2\vec{I}\; f(\vec{I})a(\vec{I})\vec{e_1} + \int_{\mathbb{S}^2} d^2\vec{I}\; f(\vec{I})b(\vec{I})\vec{e_2}\end{aligned}$$

and the fact that $\vec{n}$, $\vec{e_1}$ and $\vec{e_2}$ forms an orthonormal triad, it follows that

$$S = \int_{\mathbb{S}^2} d^2\vec{I}\; f(\vec{I})P_2(\vec{I}\cdot\vec{n}) \tag{5}$$

We have that $P_{2|[-1;1]}(x)$ is a parabola with a minimum in 0 and equal maximum in -1 and 1, therefore we can interpret S in Equation 5 as a measure of how well the particles are aligned with $\vec{n}$. We can also notice that in an isotropic phase for which f is a flat probability distribution, $f(\vec{I}) = f_0 = 1/4\pi$ with Equation 2, we have

$$\begin{aligned}S &= \int_{\mathbb{S}^2} d^2\vec{I}\; f_0 P_2(\vec{I}\cdot\vec{n}) = \frac{1}{4\pi}\cancelto{0}{\int_{\mathbb{S}^2} d^2\vec{I}\; P_2(\vec{I}\cdot\vec{n})} \\ &= 0\end{aligned}$$

thus indicating that $S = 0$ for an isotropic phase. We have then finally showed that S is the correct nematic order parameter associated to the director $\vec{n}$.

1.2 Nematic order in static packings of spheroids

We want to investigate the existence of a nematic order in static packings of spheroids. This investigation has recently been led by Nascimento *et al.* [16], also inspired by the work of Onsager. We will here develop their calculations and perform the relevant numerical calculations.

1.2.1 Free energy

The first step to our journey is to calculate the free energy F – or equivalently the free energy density $\mathcal{F} = F/V$ with V the volume of the system – of the packing as a function of the probability distribution of orientation f, so that the minimisation of F – or $\mathcal{F}$ – will enable us to determine f and consequently the nematic order parameter S.

Consider N identical spheroids in a volume V, we will denote $\rho_0 = N/V$ the number density of the spheroids considered homogeneous in the whole packing and v_0 their volume. We consider that two spheroids i and j interact with the following potential

$$U_{ij} = \begin{cases} +\infty & \text{if } i \text{ and } j \text{ interpenetrate,} \\ 0 & \text{otherwise.} \end{cases} \tag{6}$$

modeling hard-core interactions.

Authors of [16] showed that the free energy density of the packing has the following expression within an additive constant

$$\mathcal{F} = \frac{F}{V} = -\frac{1}{\beta}\rho_0 \Bigg[-\ln\rho_0 \underbrace{- \int_{\mathbb{S}^2} d^2\vec{I}\; f(\vec{I}) \ln f(\vec{I})}_{①} + \underbrace{\int_{\mathbb{S}^2} d^2\vec{I} f(\vec{I}) \ln\left(1 - \lambda\rho_0 \int_{\mathbb{S}^2} d^2\vec{I}'\; f(\vec{I}') V_{\text{exc}}(\vec{I},\vec{I}')\right)}_{②} \Bigg] \tag{7}$$

where $V_{\text{exc}}(\vec{I},\vec{I}')$ is the pair excluded excluded volume between two spheroids with symmetry axis along $\vec{I}$ and $\vec{I}'$, and λ is a parameter which will be considered as a constant.

Equation 7 contains all the physics of the problem. Term ① represents the orientational entropy, while term ② represents the effect of excluded volume. [17] At low density, the effects of excluded volume are negligible, we thus have to maximise the orientational entropy in order to minimise the free energy, hence the isotropic phase. At higher density, when particles are more closely packed, the effects of excluded volume are predominant, particles thus have to align in order to minimise the excluded volume and minimise the free energy, hence the nematic phase. A phase transition between the isotropic and nematic is then to be expected at a given density.

We can now get on with the minimisation of the free energy. We must first provide an expression for the excluded volume. Recent work by Piastra and Virga [18], summarised in Appendix A of [16] for spheroids, showed that for spheroids with symmetry axis aligned with $\vec{I}$ and $\vec{I}'$ we can write

$$V_{\text{exc}}(\vec{I},\vec{I}') = C - \frac{2}{3} D\boldsymbol{\sigma}(\vec{I}) : \boldsymbol{\sigma}(\vec{I}') \tag{8}$$

where C and D are constants determined by the aspect ration of the spheroids and : denotes the double dot product such that

$$A = \sum_i \vec{a_i} \otimes \vec{b_i},\; B = \sum_j \vec{c_j} \otimes \vec{b_j} \Rightarrow A : B = B : A = \sum_i \sum_j (\vec{a_i} \cdot \vec{d_j})(\vec{b_i} \cdot \vec{c_j})$$

For a matter of simplicity, we will denote $c = \lambda C$ and $d = \lambda D$. We can now rewrite equation 7 as

$$\mathcal{F} = \frac{1}{\beta}\rho_0 \Bigg[\ln\rho_0 + \int_{\mathbb{S}^2} d^2\vec{I}\; f(\vec{I}) \ln f(\vec{I}) - \int_{\mathbb{S}^2} d^2\vec{I}\; f(\vec{I}) \ln\left(1 - \rho_0 \int_{\mathbb{S}^2} d^2\vec{I}'\; f(\vec{I}') \left(c - \frac{2}{3} d\boldsymbol{\sigma}(\vec{I}) : \boldsymbol{\sigma}(\vec{I}')\right)\right) \Bigg]$$

where

$$\begin{aligned} &\int_{\mathbb{S}^2} d^2\vec{I}'\; f(\vec{I}') \left(c - \frac{2}{3} d\boldsymbol{\sigma}(\vec{I}) : \boldsymbol{\sigma}(\vec{I}')\right) \\ =& c \cancel{\int_{\mathbb{S}^2} d^2\vec{I}'\; f(\vec{I}')}^{\,1} - \frac{2}{3} d\boldsymbol{\sigma}(\vec{I}) : \underbrace{\int_{\mathbb{S}^2} d^2\vec{I}'\; f(\vec{I}') \boldsymbol{\sigma}(\vec{I}')}_{=\boldsymbol{Q}} \end{aligned}$$

then, with the following dimensionless parameter

$$\phi = \frac{\rho_0 c - 1}{\rho_0 d} \tag{9}$$

introduced in [16], we finally get

$$\mathcal{F} = \frac{1}{\beta}\rho_0 \Bigg[\ln\rho_0 + \int_{\mathbb{S}^2} d^2\vec{I}\; f(\vec{I}) \ln f(\vec{I}) - \int_{\mathbb{S}^2} d^2\vec{I}\; f(\vec{I}) \ln\left(\frac{2}{3}\boldsymbol{\sigma}(\vec{I}) : \int_{\mathbb{S}^2} d^2\vec{I}'\; f(\vec{I}') \boldsymbol{\sigma}(\vec{I}') - \phi\right) \Bigg] \tag{10}$$

which has to be minimised with respect to $f(\vec{I})$ with the constraint of Equation 2 written as

$$\mathcal{G} = \int_{\mathbb{S}^2} d^2\vec{I}\; f(\vec{I}) - 1 = 0 \tag{11}$$

Therefore, if $f(\vec{I})$ minimises $\mathcal{F}$, we have for any infinitely small $\delta f(\vec{I})$

$$\mathcal{F}\left(f(\vec{I}) + \delta f(\vec{I})\right) - \mathcal{F}\left(f(\vec{I})\right) + \mu\left(\mathcal{G}\left(f(\vec{I}) + \delta f(\vec{I})\right) - \mathcal{G}\left(f(\vec{I})\right)\right) = 0 \tag{12}$$

where μ is a Lagrange multiplier.

We have

$$\begin{aligned}
&\int_{\mathbb{S}^2} d^2\vec{I}\; (f(\vec{I}) + \delta f(\vec{I}))\ln(f(\vec{I}) + \delta f(\vec{I})) - \int_{\mathbb{S}^2} d^2\vec{I}\; f(\vec{I})\ln f(\vec{I}) \\
=&\int_{\mathbb{S}^2} d^2\vec{I}\; \delta f(\vec{I})(\ln f(\vec{I}) + 1)
\end{aligned}$$

and within an additional term of order $\mathcal{O}(\delta f^2)$

$$\begin{aligned}
&\int_{\mathbb{S}^2} d^2\vec{I}\; (f(\vec{I}) + \delta f(\vec{I}))\ln\left(\frac{2}{3}\boldsymbol{\sigma}(\vec{I}) : \int_{\mathbb{S}^2} d^2\vec{I'}\; (f(\vec{I'}) + \delta f(\vec{I'}))\boldsymbol{\sigma}(\vec{I'}) - \phi\right) \\
&- \int_{\mathbb{S}^2} d^2\vec{I}\; f(\vec{I})\ln\left(\frac{2}{3}\boldsymbol{\sigma}(\vec{I}) : \int_{\mathbb{S}^2} d^2\vec{I'}\; f(\vec{I'})\boldsymbol{\sigma}(\vec{I'}) - \phi\right) \\
=&\int_{\mathbb{S}^2} d^2\vec{I}\; \delta f(\vec{I})\ln\left(\frac{2}{3}\boldsymbol{\sigma}(\vec{I}) : \underbrace{\int_{\mathbb{S}^2} d^2\vec{I'}\; f(\vec{I'})\boldsymbol{\sigma}(\vec{I'})}_{\boldsymbol{Q}} - \phi\right) \\
&+ \int_{\mathbb{S}^2} d^2\vec{I}\; \delta f(\vec{I})\boldsymbol{\sigma}(\vec{I}) : \left(\int_{\mathbb{S}^2} d^2\vec{I'}\; f(\vec{I'})\frac{\frac{2}{3}\boldsymbol{\sigma}(\vec{I'})}{\frac{2}{3}\boldsymbol{\sigma}(\vec{I'}) : \underbrace{\int_{\mathbb{S}^2} d^2\vec{I''}\; f(\vec{I''})\boldsymbol{\sigma}(\vec{I''})}_{\boldsymbol{Q}} - \phi}\right)
\end{aligned}$$

and finally

$$\mathcal{G}\left(f(\vec{I}) + \delta f(\vec{I})\right) - \mathcal{G}\left(f(\vec{I})\right) = \int_{\mathbb{S}^2} d^2\vec{I}\; \delta f(\vec{I})$$

thus, with

$$\frac{2}{3}\boldsymbol{\sigma}(\vec{I}) : \boldsymbol{Q} = SP_2(\vec{I}\cdot\vec{n}) \tag{13}$$

Equation 12 becomes

$$\begin{aligned}
\int_{\mathbb{S}^2} d^2\vec{I}\; \delta f(\vec{I})\Bigg(&\ln f(\vec{I}) + 1 - \ln\left(SP_2(\vec{I}\cdot\vec{n}) - \phi\right) \\
&- \boldsymbol{\sigma}(\vec{I}) : \left(\int_{\mathbb{S}^2} d^2\vec{I'}\; f(\vec{I'})\frac{\frac{2}{3}\boldsymbol{\sigma}(\vec{I'})}{SP_2(\vec{I}\cdot\vec{n}) - \phi}\right) + \mu\Bigg) = 0
\end{aligned} \tag{14}$$

which has to be verified for any choice of $\delta f(\vec{I})$, implying that the part between parenthesis in the integrand must be equal to 0.

We introduce

$$\boldsymbol{\psi} = \int_{\mathbb{S}^2} d^2\vec{I}\; f(\vec{I})\frac{\frac{2}{3}\boldsymbol{\sigma}(\vec{I})}{SP_2(\vec{I}\cdot\vec{n}) - \phi} = \psi(\vec{n}\otimes\vec{n} - \frac{1}{3}\mathbb{1}) \tag{15}$$

such that

$$\boldsymbol{\sigma}(\vec{I}) : \boldsymbol{\psi} = \psi P_2(\vec{I} \cdot \vec{n})$$

and that the function $f(\vec{I})$ which satisfies Equation 14 is

$$f(\vec{I}) = \begin{cases} \frac{(SP_2(\vec{I}\cdot\vec{n})-\phi)e^{\psi P_2(\vec{I}\cdot\vec{n})}}{\int_{\mathbb{S}^2_+} d^2\vec{I}'\ (SP_2(\vec{I}'\cdot\vec{n})-\phi)e^{\psi P_2(\vec{I}'\cdot\vec{n})}} & \text{if } SP_2(\vec{I}\cdot\vec{n}) - \phi > 0, \\ 0 & \text{otherwise.} \end{cases} \tag{16}$$

where $\mathbb{S}^2_+ = \{\vec{I} \in \mathbb{S}^2,\ SP_2(\vec{I}\cdot\vec{n}) - \phi > 0\}$. We have that the only relevant variable is $x \equiv \vec{I}\cdot\vec{n}$, therefore by integration over the other components of $\vec{I}$ and by noticing that the integrand in the denominator is an even function of x, we get

$$f(x) = \frac{1}{4\pi} \begin{cases} \frac{(SP_2(x)-\phi)e^{\psi P_2(x)}}{\int_{S_+} dx'\ (SP_2(x')-\phi)e^{\psi P_2(x')}} & \text{if } SP_2(x) - \phi > 0, \\ 0 & \text{otherwise.} \end{cases} \tag{17}$$

where $S_+ = \{x \in [0;1], SP_2(x) - \phi > 0\}$. Rather than solving this self-consistent equation for $f(x)$, we use Equations 5 and 15 in Equation 17, and with x_0 the positive root of

$$SP_2(x_0) - \phi = 0 \tag{18}$$

we write

$$S = \frac{\int_{S_+} dx\ P_2(x)(P_2(x) - P_2(x_0))e^{\psi P_2(x)}}{\int_{S_+} dx\ (P_2(x) - P_2(x_0))e^{\psi P_2(x)}} \tag{19}$$

$$\frac{1}{\psi} = \frac{\int_{S_+} dx\ P_2^2(x)e^{\psi P_2(x)}}{\int_{S_+} dx\ P_2(x)e^{\psi P_2(x)}} - P_2(x_0) \tag{20}$$

for which S_+ is then given by

$$S_+ = \begin{cases} [x_0;1] & \text{if } S > 0, \\ [0;x_0] & \text{if } S < 0. \end{cases}$$

1.2.2 Equilibrium nematic order parameter

To get the equilibrium nematic order parameter S as a function of the order parameter $\phi(\rho_0)$, we take a $\psi \in]-\infty;+\infty[$ and solve Equation 20 for x_0, then find the corresponding $S > 0$ and $S < 0$ with Equation 19 and finally the corresponding ϕ with Equation 18.

To determine the stability of the equilibrium solutions, we need to know for each ϕ the local convexity of the free energy in the vicinity of the corresponding equilibrium nematic order parameters $S^*(\phi)$. Let us first notice with Equation 16 that

$$\int_{\mathbb{S}^2} d^2\vec{I}\ f(\vec{I}) \ln f(\vec{I}) = \underbrace{\int_{\mathbb{S}^2_+} d^2\vec{I}\ f(\vec{I})\psi P_2(\vec{I}\cdot\vec{n})}_{\psi S} + \int_{\mathbb{S}^2_+} d^2\vec{I}\ f(\vec{I}) \ln(SP_2(\vec{I}\cdot\vec{n}) - \phi)$$
$$\underbrace{- \int_{\mathbb{S}^2} d^2\vec{I}\ f(\vec{I}) \ln \int_{\mathbb{S}^2_+} d^2\vec{I}'\ (SP_2(\vec{I}'\cdot\vec{n}) - \phi)e^{\psi P_2(\vec{I}'\cdot\vec{n})}}_{\ln \int_{\mathbb{S}^2_+} d^2\vec{I}'\ (SP_2(\vec{I}'\cdot\vec{n})-\phi)e^{\psi P_2(\vec{I}'\cdot\vec{n})}}$$

Therefore, with Equations 10 and 13, we have the following expression within an additive constant for the free energy density

$$\mathcal{F} = \frac{1}{\beta}\rho_0 \left(\psi S - \ln \int_{\mathbb{S}^2_+} d^2\vec{I}\ (SP_2(\vec{I}\cdot\vec{n}) - \phi)e^{\psi P_2(\vec{I}\cdot\vec{n})} \right) \tag{21}$$

We can then compute the first and second partial derivatives of $\mathcal{F}$ with respect to S to determine the stability of the solutions.

We solved the minimisation equation for $\mathcal{F}$, determined the couples (ϕ, S) of equilibrium solutions and computed the local convexity of $\mathcal{F}$ with Wolfram MATHEMATICA. All the code which has been developed for this task is available on the GitHub repository yketa/M2_PT_project. We are mainly interested in stable solutions with $S > 0$, therefore we only show here the results for the conditions $S > 0$ and $\psi \in]0; +\infty[$, and $S = 0$ and $\psi = 0$ which is also an equilibrium solution $\forall \phi < 0$ according to equations 19 and 20. Results are presented in Figure 2.

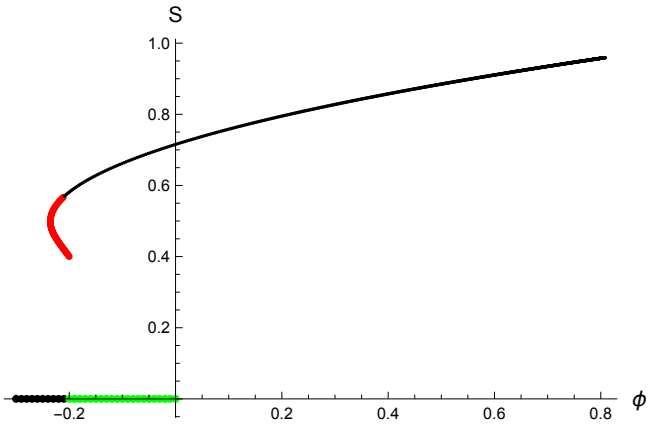

Figure 2: Nematic order parameter S as a function of ϕ. Black curves represent stable states, red curve represents metastable states and green curve represents unstable states.

From our data, we get that the stable solution for $\phi < \phi_{NI} \sim -0.211$ is $S = 0$ while the stable solution for $\phi > \phi_{NI}$ is $S > S_{NI} \sim 0.567$. Therefore, there is a phase transition at $\phi = \phi_{NI}$ between an isotropic and a nematic phase. There is a discontinuity in the order parameter S at this transition, which is then a first-order phase transition.

Our results are a bit different from the paper, where the authors got $\phi_{NI,\text{th.}} = -0.224$ and $S_{NI,\text{th.}} = 0.545$. Moreover, we do not observe a metastable part in the $S > 0$ curve. We believe these differences are due to numerical errors in the successive operations we have performed.

2 Nematic order close to the jamming transition

We have in the study of Nascimento *et al.* [16] that the nematic order of the static packing of spheroids tends to 1 when increasing its density. Therefore, their densest packing possible is a crystal array, as in [11].

However, it has been reported that no orientational order is present at jamming [9, 10]. In order to investigate this, we will here report on shearing simulations conducted on packings of soft-core frictionless spheroids with harmonic repulsive interaction. In these simulations, the control parameters relevant to the jamming transition are the packing fraction ϕ and the shear rate $\dot{\gamma}$.

2.1 Jamming as a critical phenomenon

2.1.1 Critical behaviour

In the vicinity of the jamming transition, we have that the shear viscosity $\eta \equiv \sigma/\dot{\gamma}$ – with σ the shear stress and $\dot{\gamma}$ the shear strain rate, – or equivalently the pressure viscosity $\eta_p \equiv p/\dot{\gamma}$ – with p the pressure, – and a correlation length scale ξ diverge as

$$\begin{aligned} \eta, \eta_p &\underset{\phi \to \phi_J}{\sim} (\phi_J - \phi)^{-\beta} \\ \xi &\underset{\phi \to \phi_J}{\sim} (\phi_J - \phi)^{-\nu} \end{aligned} \tag{22}$$

for soft-core particles in the limit $\dot{\gamma} \to 0$ [7, 19] and for hard-core particles [20]. This power-law divergence of the transport coefficient and of a correlation length scale are reminiscent of the behaviour near a critical point [19, 21, 22] of a second-order continuous phase transition.

2.1.2 Scaling analysis

Because the pressure viscosity varies on a larger interval than the nematic order parameter, we will perform our scaling analysis on the former. We detail here how what they consist of.

Renormalisation group theory suggests that for an infinite system close to the jamming point, *i.e.* ($\phi_J - \phi = \delta\phi \to 0, \dot{\gamma} \to 0$), there exists $y_{\delta\phi}$ and $y_{\dot{\gamma}}$ such that the correlation length transforms under a change of length scale with a factor l as

$$\xi(\delta\phi, \dot{\gamma}) = l\xi(\delta\phi l^{y_{\delta\phi}}, \dot{\gamma} l^{y_{\dot{\gamma}}})$$

which, when choosing l such that $\delta\phi l^{y_{\delta\phi}} = b \Leftrightarrow l = \left(\frac{\delta\phi}{b}\right)^{-1/y_{\delta\phi}} \geq 1$, gives

$$\xi(\delta\phi, \dot{\gamma}) = \left(\frac{\delta\phi}{b}\right)^{-1/y_{\delta\phi}} \xi\left(b, \dot{\gamma}\left(\frac{\delta\phi}{b}\right)^{-y_{\dot{\gamma}}/y_{\delta\phi}}\right) \underset{\delta\phi\to 0}{\sim} (\delta\phi)^{-1/y_{\delta\phi}}$$

where we recognise $\nu = 1/y_{\delta\phi} > 0$ according to equation 22.

We will assume that variables which vanish at jamming are somehow linked to the free energy density of the system. Therefore, in accordance with renormalisation group theory, we here suggest the following assumption on the scaling of a vanishing variable $\mathcal{O}$ close to the jamming point for a change of length scale with a factor l

$$\mathcal{O}(\delta\phi, \dot{\gamma}) \sim l^{-y_{\mathcal{O}}/\nu} g_{\mathcal{O}}(\delta\phi l^{1/\nu}, \dot{\gamma} l^{z}) \tag{23}$$

where we can choose $\delta\phi l^{1/\nu} = b \Leftrightarrow l = \left(\frac{\delta\phi}{b}\right)^{-\nu} \geq 1$ and deduce

$$\mathcal{O}(\delta\phi, \dot{\gamma}) \sim \left(\frac{\delta\phi}{b}\right)^{y_{\mathcal{O}}} g_{\mathcal{O}}\left(b, \dot{\gamma}\left(\frac{\delta\phi}{b}\right)^{-\nu z}\right)$$

where we take the $\delta\phi \to 0$ limit, which gives

$$\mathcal{O}(\delta\phi, \dot{\gamma}) \underset{\delta\phi\to 0}{\sim} (\delta\phi)^{y_{\mathcal{O}}} \tag{24}$$

with $y_{\mathcal{O}} > 0$ thus being the critical exponent associated to the vanishing of the variable $\mathcal{O}$ at jamming.

We introduce the function $\tilde{g}_p$ such that equation 23 applied to the pressure p can be written

$$p(\delta\phi, \dot{\gamma}) \sim \dot{\gamma} l^z l^{-y_p/\nu} \tilde{g}_p(\delta\phi l^{1/\nu}, \dot{\gamma} l^z)$$

and then choose l such that $\delta\phi l^{1/\nu} = b \Leftrightarrow l = \left(\frac{\delta\phi}{b}\right)^{-\nu} \geq 1$, which leads to

$$p(\delta\phi, \dot{\gamma}) \sim \dot{\gamma}\left(\frac{\delta\phi}{b}\right)^{-(\nu z - y)} \tilde{g}_p\left(b, \dot{\gamma}\left(\frac{\delta\phi}{b}\right)^{-\nu z}\right)$$

and therefore

$$\eta_p(\delta\phi, \dot{\gamma}) \equiv p(\delta\phi, \dot{\gamma})/\dot{\gamma} \underset{\delta\phi\to 0}{\sim} (\delta\phi)^{-(\nu z - y)} \tag{25}$$

where we recognise $\beta = \nu z - y$ according to equation 22.

We now choose l such that $\dot{\gamma} l^z = b \Leftrightarrow l = \left(\frac{\dot{\gamma}}{b}\right)^{-1/z} \geq 1$, which put in equation 23 for p leads to

$$p(\delta\phi, \dot{\gamma}) \sim \dot{\gamma}^{y_p/\nu z} g_p \left(\delta\phi \left(\frac{\dot{\gamma}}{b}\right)^{-1/\nu z}, b \right)$$

and finally introduce the function $g_p^{(\text{fit})}$ in order to ignore the constant b in this last equation, which becomes

$$p(\delta\phi, \dot{\gamma}) \sim \dot{\gamma}^{y_p/\nu z} g_p^{(\text{fit})}(\delta\phi \dot{\gamma}^{-1/\nu z}) \tag{26}$$

and in which we will denote $q_p \equiv y_p/\nu z$ and $h_p \equiv -1/\nu z$, thus leading to $\beta = (q_p - 1)/h_p$, in addition to $Y_p \equiv p(\delta\phi, \dot{\gamma})\dot{\gamma}^{-q_p}$ and $X_p \equiv \delta\phi\dot{\gamma}^{h_p}$.

Equation 26 suggests that it is possible to collapse the data from simulations at different packing fractions and shear strain rates on a single curve in the (X_p,Y_p) plane. To perform this fitting, we choose arbitrarily the expression of $g_{\mathcal{O}}^{(\text{fit})}$

$$g_p^{(\text{fit})} : X_p \mapsto \exp\left(\sum_{i=0}^{5} a_{p,i} X_p^i \right)$$

and use the Levenberg-Marquardt algorithm [23, 24] with ϕ_J, z_c, q_p, h_p and $a_{p,0}$ through $a_{p,5}$ as free parameters.

2.1.3 Soft- to hard-core mapping

Shearing simulations are more easily conducted with soft-core particles. However, we are interested in the behaviour of hard-core packings near jamming, we thus have to remove the effect of the particles interpenetration in our data.

We can find in [20] a method to map soft-core particles at a given packing fraction ϕ and shear strain rate $\dot{\gamma}$ to equivalent hard-core particles at a lesser packing fraction ϕ_{eff} such as

$$\begin{aligned} \eta_p^s(\phi, \dot{\gamma}) &= \eta_p^s(\phi_{\text{eff}}, \dot{\gamma} \to 0) \\ \eta_p^h(\phi_{\text{eff}}) \equiv \eta_p^s(\phi_{\text{eff}}, \dot{\gamma} \to 0) &\underset{\phi_{\text{eff}} \to \phi_J}{\sim} (\phi_J - \phi_{\text{eff}})^{-\beta} \end{aligned} \tag{27}$$

according to equation 22.

This mapping is done by assuming that ϕ_{eff} is determined by the extent of particle overlaps, measured by the average energy per particle $E(\phi, \dot{\gamma})$. Authors of [20] then proposed the following relation

$$\phi_{\text{eff}}(\phi, \dot{\gamma}) = \phi - h(E(\phi, \dot{\gamma})) \tag{28}$$

where h can be determined asymptotically close to ϕ_J. Indeed, further considerations on the jamming transition gives us the following expression

$$\phi_{\text{eff}}(\phi, \dot{\gamma}) \underset{\phi \to \phi_J}{=} \phi - cE(\phi, \dot{\gamma})^{1/y_E} \tag{29}$$

with c a constant.

In our model of harmonic elastic interactions, the pressure and the energy scale as $E \sim p^2$. Therefore, we have that y_E satifies the following relation

$$y_E = 2y_p \Leftrightarrow y_E = -2q_p/h_p \tag{30}$$

Therefore, considering that q_p and h_p have been determined with our scaling method, c remains the only unknown variable in equation 29.

Equations 27 and 29 can be rewritten as

$$\eta_p^s(\phi,\dot{\gamma}) = A\left(\phi_J - \phi + cE(\phi,\dot{\gamma})^{-h_p/2q_p}\right)^{-\beta} \tag{31}$$

where A is an additional parameter which can be determined if we take two points $\eta_{p,1} \equiv \eta_p(\phi_1,\dot{\gamma}_1)$ and $\eta_{p,2} \equiv \eta_p(\phi_2,\dot{\gamma}_2)$, whose corresponding energies are $E_1 \equiv E(\phi_1,\dot{\gamma}_1)$ and $E_2 \equiv E(\phi_2,\dot{\gamma}_2)$, which we hypothesise satisfy equation 31. We can then isolate c in equation 31, giving

$$c = E(\phi,\dot{\gamma})^{h_p/2q_p}\left(A^{1/\beta}\eta_p(\phi,\dot{\gamma})^{-1/\beta} - \phi_J + \phi\right)$$

which has to be satisfied by the two aforementioned points, therefore

$$\begin{aligned} &E_1^{h_p/2q_p}\left(A^{1/\beta}\eta_{p,1}^{-1/\beta} - \phi_J + \phi_1\right) = E_2^{h_p/2q_p}\left(A^{1/\beta}\eta_{p,2}^{-1/\beta} - \phi_J + \phi_2\right) \\ \Leftrightarrow &A = \left(\left(\eta_{p,1}^{-1/\beta}E_1^{h_p/2q_p} - \eta_{p,2}^{-1/\beta}E_2^{h_p/2q_p}\right)^{-1}\left(E_1^{h_p/2q_p}(\phi_J - \phi_1) + E_2^{h_p/2q_p}(\phi_2 - \phi_J)\right)\right)^{\beta} \end{aligned}$$

which can be re-injected in the expression of c evaluated in either point.

This method enables us to do two things:

- Verify that the data for an other variable than the pressure is consistent with the latter. Indeed, if everything is consistent, we will see that the curves for different shear rates will collapse on a single curve.
- Find the critical exponent associated to the vanishing of an other variable than the pressure with a simple linear regression rather than with the scaling analysis we have described.

2.2 Nematic order

We present here our results on the nematic order parameter S in shearing simulations of spheroids in Figure 3.

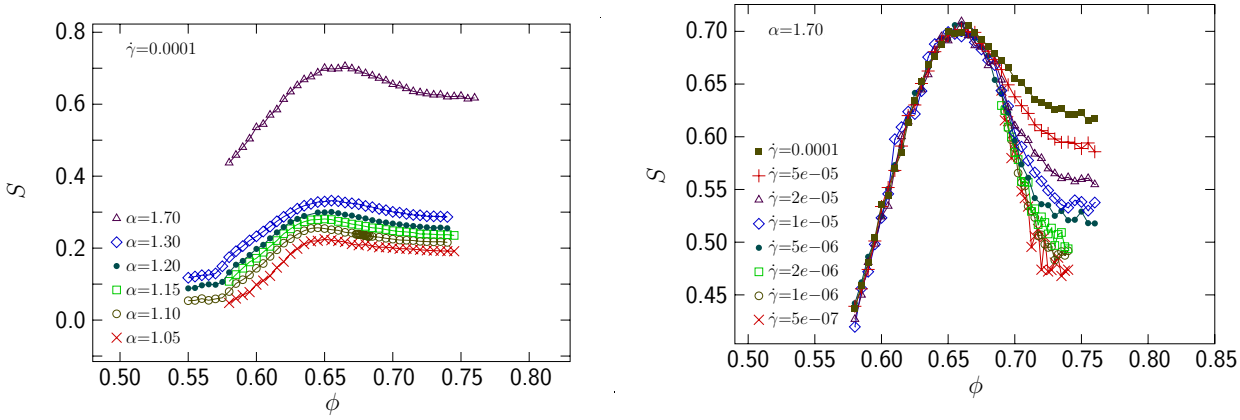

(a) Different aspect ratio and same shear rate.

(b) Same aspect ration and different shear rate.

Figure 3: Nematic order parameter S as a function of the packing fraction ϕ.

We first observe that we always have a strictly positive S, *i.e.* the system can never be described as an isotropic phase. Contrarily to the static packings we first studied in this essay, the isotropy of space is here broken by the shearing, such a result was then to be expected. Indeed, shear-alignment of anisotropic particles have already been reported. [25] However, data at very low packing fractions where particles seldom come into contact, and thus are very little influenced by the shearing, could give a negligible nematic order parameter. In addition, we have regions of ϕ where S is lesser than $S_{NI,\text{th.}}$, which is the minimum S theoretically obtained for static packings. This also suggests that the origin of the orientational ordering in our sheared packings is different from its origin in static packings.

There is a first domain of packing fractions where S is an increasing function of the packing fraction at fixed aspect ratio and where it does not depend on the shear rate, hence suggesting that this behaviour is linked to static – rather than dynamic – properties of the packings. It can be explained by the depletion of available orientation configurations with increasing packing fraction: the particles tend to align to decrease the excluded volume effect as we have seen before. This is consistent with S being an increasing function of the aspect ratio at fixed packing fraction since the effects of excluded volumes increase with increasing aspect ratio.

We then have that S reaches a maximum for a particular packing fraction before decreasing near the jamming density. This is the part we are interested in.

We apply the soft- to hard-core mapping technique we have presented to the nematic order parameter S. We see that data for different shear rates collapse on a single curve, hence showing that the data for S is consistent with the data for p. We can then proceed to the linear regression in order to determine if, in the vicinity of the jamming transition, S decreases algebraically with the distance to the jamming packing fraction as we would expect near a critical point. Results are presented in Figure 4.

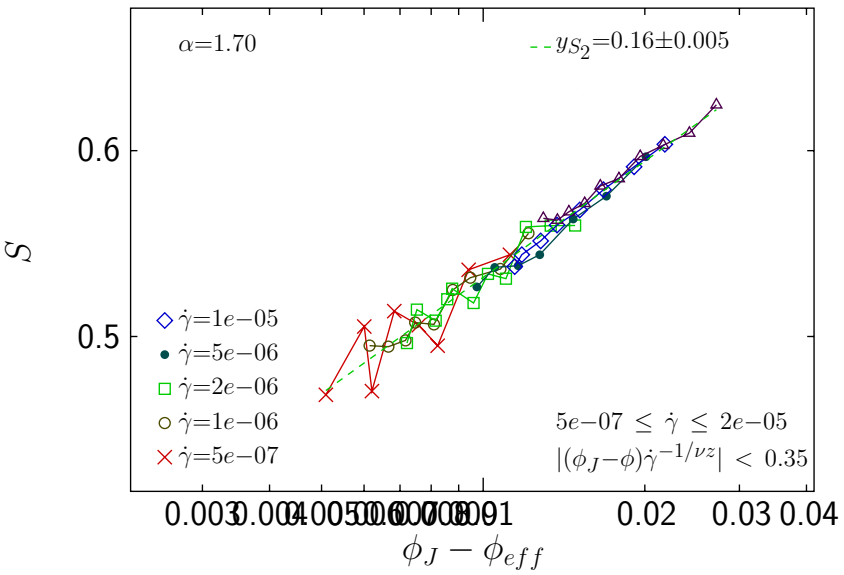

Figure 4: Nematic order parameter S as a function of the effective packing fraction ϕ_{eff}.

Our data then shows evidence for a critical vanishing of the nematic order parameter S at the jamming transition which is consistent with the vanishing of the pressure. Despite the low error on the critical exponent, we still need more data closer to the jamming density to give a quantitative result.

Conclusion

In this essay, we have studied the orientational order of packings of anisotropic particles, here spheroids.

First, we have detailed the calculations of the recent paper by Nascimento *et al.* [16], and determined the equilibrium nematic order parameter S in static packings of hard-core spheroids. In accordance with the findings of [16], we have showed that such packings experience a first-order phase transition between a disordered, isotropic, phase and an orderered, anisotropic, phase. This transition occurs at a packing fraction which is a function of the aspect ratio of the spheroids. Futher inquieries are necessary to determine the possibility of coexistence between isotropic and nematic phases.

Then, after reminding that the jamming transition is a second-order phase transition, we have showed that

sheared packings of soft-core spheroids display an orientational order at packing fractions lesser than the jamming density but that this order, measured with the nematic order parameter S, vanishes algebraically at jamming in accordance with the critical vanishing of the pressure. Further inquiries are necessary, first to find out what drives this transition from a nematic to an isotropic phase, and second to determine if the critical exponent associated to S depends on the aspect ratio of the spheroids.

Acknowledgements

I wish to thank Peter Olsson, Guilhem Poy, Nicolas Taberlet, Valérie Vidal and Jean-Christophe Geminard for (very) helpful discussions. I also wish to thank Jean-Rémy Conti for the long days of work we had together.

References

[1] Jacques Duran. *Sands, powders, and grains: an introduction to the physics of granular materials*. Springer Science & Business Media, 2012.

[2] Richard Patrick, Mario Nicodemi, Renaud Delannay, Philippe Ribiere, and Daniel Bideau. Slow relaxation and compaction of granular systems. *Nature materials*, 4(2):121, 2005.

[3] Pierre-Gilles de Gennes. Granular matter: a tentative view. *Reviews of modern physics*, 71(2):S374, 1999.

[4] Leo P Kadanoff. Built upon sand: Theoretical ideas inspired by granular flows. *Reviews of Modern Physics*, 71(1):435, 1999.

[5] Corey S O'hern, Leonardo E Silbert, Andrea J Liu, and Sidney R Nagel. Jamming at zero temperature and zero applied stress: The epitome of disorder. *Physical Review E*, 68(1):011306, 2003.

[6] Hugo Jacquin, Ludovic Berthier, and Francesco Zamponi. Microscopic mean-field theory of the jamming transition. *Physical review letters*, 106(13):135702, 2011.

[7] Peter Olsson and Stephen Teitel. Critical scaling of shear viscosity at the jamming transition. *Physical review letters*, 99(17):178001, 2007.

[8] Daniel Vågberg, Peter Olsson, and Stephen Teitel. Glassiness, rigidity, and jamming of frictionless soft core disks. *Physical Review E*, 83(3):031307, 2011.

[9] Aleksandar Donev, Ibrahim Cisse, David Sachs, Evan A Variano, Frank H Stillinger, Robert Connelly, Salvatore Torquato, and Paul M Chaikin. Improving the density of jammed disordered packings using ellipsoids. *Science*, 303(5660):990–993, 2004.

[10] Weining Man, Aleksandar Donev, Frank H Stillinger, Matthew T Sullivan, William B Russel, David Heeger, Souheil Inati, Salvatore Torquato, and PM Chaikin. Experiments on random packings of ellipsoids. *Physical review letters*, 94(19):198001, 2005.

[11] Aleksandar Donev, Frank H Stillinger, PM Chaikin, and Salvatore Torquato. Unusually dense crystal packings of ellipsoids. *Physical review letters*, 92(25):255506, 2004.

[12] PM Chaikin, Aleksandar Donev, Weining Man, Frank H Stillinger, and Salvatore Torquato. Some observations on the random packing of hard ellipsoids. *Industrial & engineering chemistry research*, 45(21): 6960–6965, 2006.

[13] D Frenkel and BM Mulder. The hard ellipsoid-of-revolution fluid: I. monte carlo simulations. *Molecular physics*, 55(5):1171–1192, 1985.

[14] Lars Onsager. The effects of shape on the interaction of colloidal particles. *Annals of the New York Academy of Sciences*, 51(1):627–659, 1949.

[15] Anupam Sengupta. *Topological microfluidics: nematic liquid crystals and nematic colloids in microfluidic environment*. Springer Science & Business Media, 2013.

[16] Eduardo S Nascimento, Peter Palffy-Muhoray, Jamie M Taylor, Epifanio G Virga, and Xiaoyu Zheng. Density functional theory for dense nematic liquid crystals with steric interactions. *Physical Review E*, 96 (2):022704, 2017.

[17] E Priestly. *Introduction to liquid crystals*. Springer Science & Business Media, 2012.

[18] Marco Piastra and Epifanio G Virga. Explicit excluded volume of cylindrically symmetric convex bodies. *Physical Review E*, 91(6):062503, 2015.

[19] Peter Olsson and S Teitel. Critical scaling of shearing rheology at the jamming transition of soft-core frictionless disks. *Physical Review E*, 83(3):030302, 2011.

[20] Peter Olsson and S Teitel. Herschel-bulkley shearing rheology near the athermal jamming transition. *Physical review letters*, 109(10):108001, 2012.

[21] Michael Plischke and Birger Bergersen. *Equilibrium statistical physics*. World Scientific Publishing Co Inc, 1994.

[22] Daniel Vågberg, Daniel Valdez-Balderas, MA Moore, Peter Olsson, and Stephen Teitel. Finite-size scaling at the jamming transition: Corrections to scaling and the correlation-length critical exponent. *Physical Review E*, 83(3):030303, 2011.

[23] Donald W Marquardt. An algorithm for least-squares estimation of nonlinear parameters. *Journal of the society for Industrial and Applied Mathematics*, 11(2):431–441, 1963.

[24] William H Press. *Numerical recipes 3rd edition: The art of scientific computing*. Cambridge university press, 2007.

[25] Tamás Börzsönyi, Balázs Szabó, Gábor Törös, Sandra Wegner, János Török, Ellák Somfai, Tomasz Bien, and Ralf Stannarius. Orientational order and alignment of elongated particles induced by shear. *Physical review letters*, 108(22):228302, 2012.